Ultrasound Assisted Synthesis of Nanoscale NH_2-MIL-53(Fe) for the Adsorption of Dye①

WU Xue-Min[a, b] LIU Long-Xue[a] LIU Ling[a]
YOU Zi-Han[a] GUO Hong-Xu[a, b②] CHEN Zhang-Xu[b②]
[a] (*College of Chemistry, Chemical Engineering and Environment, Minnan Normal University, Zhangzhou* 363000, *China*)
[b] (*Fujian Provincial Key Laboratory of Ecology-toxicological Effects & Control for Emerging Contaminants, Putian University* 351100, *China*)

ABSTRACT Nanometer blocks of amide-functionalized Fe(Ⅲ)-based metal-organic frameworks, NH_2-MIL-53(Fe), were prepared *via* ultrasonic method without any surfactants at room temperature and atmospheric pressure. The characterization for the as-prepared nano-structured MOFs was established by XRD, SEM, TEM, XPS and N_2 adsorption-desorption. The as-prepared sample with high specific surface area (179.9 $m^2\ g^{-1}$) showed excellent adsorption for methylene blue in the liquid phase. The as-prepared NH_2-MIL-53(Fe) adsorbent seems to be a promising material in practice for organic dye removal from aqueous solution.

Keywords: NH_2-MIL-53(Fe), ultrasonic method, removal, methylene blue;
DOI: 10.14102/j.cnki.0254–5861.2011–2763

1 INTRODUCTION

The presence of dyes in effluents is a major concern due to their potential to cause adverse effects to flora, fauna and humans. Complex aromatic structures and xenobiotic properties of dyes make them more difficult to degrade[1]. Methylene blue (MB), a cationic dye, has been widely used in dying cotton, wood, and silk. What we should be concerned about is the possible harm caused by the inhalation of MB, which are not only eye burns, but also vomiting, nausea, profuse sweating, painful micturition, mental confusion, and methemoglobinemia if inhaled.

At present, many methods have been developed in the decoloration of MB, such as adsorption, precipitation, reverse osmosis and ionexchange[2]. Among these possible techniques, adsorption is one of the most attractive approaches due to its low cost, versatility and ease operation[3-5]. A variety of materials capable of removing MB have been reported. Traditional absorbent materials have limitations in their application such as low adsorption capacity or difficult separation. Therefore, an efficient and economical absorbent is needed, which has the characteristics of large capacity, fast adsorption and easy separation, and can remove organic dyes in wastewater[6].

Metal-organic frameworks (MOFs) are a new class of porous crystalline hybrid materials that have achieved tremendous attention in the last decades due to those high surface area, open metal sites and large void space[7]. In the past five years, MOFs materials have been widely concerned as adsorbents for the rapid and effective removal of organic pollutants, and a large number of research results show that those are potential absorbent materials[8-10].

MOFs have been traditionally synthesized either at room temperature[11] or via a hydrothermal/solvothermal approach[12-14], usually by using an autoclave at high temperature, for a prolonged time of hours or even days. Recently, several new methods have arisen to avoid these conditions. Sonochemistry is a fast developing branch of chemistry, which takes advantage of the ultrasound (US) power. In comparison with the conventional energy sources (e.g. electrical heating), US has been proven superior in terms of simplicity, reduced reaction times and energy efficiency[15].

Received 12 February 2020; accepted 30 June 2020
① Supported by the Fujian Provincial Key Laboratory of ecotoxicological effects and Control of New pollutants (PY19001) and the Innovation and Entrepreneurship training Program for College students in 2019 (201910402063)
② Corresponding authors. Professor Guo Hong-Xu, E-mail: guohx@mnnu.edu.cn; and Dr. Chen Zhang-Xu, E-mail: xuzhangchen@163.com

Considering the production of adsorbents, the synthesis of nanometer MOF materials by simple ultrasonic method has important research value and practical application prospect[16].

In this work, amino-functionalized Fe-MOFs, block NH_2-MIL-53(Fe), as adsorbents were fabricated through a facile one-pot ecologically-friendly ultrasonic method under atmospheric pressure. The as-prepared organic-inorganic hybrid material was then characterized *via* X-ray diffraction (XRD), scanning electron microscopy (SEM), and X-ray photoelectron spectroscopy (XPS) and N_2 adsorption-desorption BET. The as-prepared sample was then employed as absorbents for the removal of MB as model organic pollutant. This study reports the development of a novel MOF-based absorbent prepared from simple ultrasonic method that can remove MB in aqueous solution.

2 EXPERIMENTAL

2. 1 Chemical reagents

All the reagents and solvents employed were commercially available and used as supplied without further purification. $Fe(NO_3)_3$ $9H_2O$ and 2-aminoterephthalic acid (H_2BDC-NH_2) (Aladdin Chemistry Co. Ltd., Shanghai, China), N,N-dimethylformamide (DMF) and ethanol (Sinopharm Chemical Reagent Co., Ltd). MB was obtained from Xilong Chemical Co., LTD (Guangdong, China).

2. 2 Preparation of block NH_2-MIL-53(Fe)

Reactants were separately prepared by dissolving 2 mmol of $Fe(NO_3)_3$ $9H_2O$ in 30 mL H_2O and 3 mmol of H_2BDC-NH_2 in 10 mL DMF. The two solutions were mixed and positioned in a highdensity ultrasonic probe at atmospheric pressure for 1 h under the temperature condition of 80 ℃, operating with a power output of 305 W. The resulting reddish brown solid powders were filtered and repeatedly washed with deionized water (20 mL × 3) and ethanol (20 mL × 3) in air. The powders were then completely dried by heating at 100 ℃ for 12 h and used as adsorbents.

2. 3 Characterization methods

XRD patterns were collected on a Rigaku D/MAX-RB diffractometer with monochromatized Cu$K\alpha$ radiation (λ = 1.5418 Å). The generator was operated at 40 kV and 25 mA. Samples were measured at diffraction angles ranging between 10 and 80 ° at a scanning rate of 0.068 ° s^{-1}. The microstructure and morphology of the as-prepared sample were examined by using scanning electron microscopy (SEM, JEOL JSM-6010). XPS tests were carried out in an ultrahigh vacuum using an ESCALAB Mark II X-ray photoelectron spectrometer (XPS, VG Scientific, UK) with Mg$K\alpha$ radiation (1253.6 eV) from the Mg anode source. High-resolution scans of the core level spectra were recorded with an energy step of 0.05 eV, and the pass energy was set up to 15 eV. The binding energy at 284.6 eV was referenced to the C1*s* peak. Experimental data were deconvolved by Gaussian-Lorentzian mixture peak-fitting software. The Brunauer-Emmett-Teller (BET) specific surface area was experimented by a multipoint BET method using the adsorption data in the relative pressure (P/P_o) range of 0.05 ～ 0.21, in which a N_2 gas was adsorption-desorption at 77 K using a Micromeritics V-Sorb 2800 P system. The sample was degassed at 180 ℃ vacuum treatment 4 h prior to BET measurements.

2. 4 Absorptive experiments

The adsorption experiment of MB was carried out under room temperature. In the adsorption kinetics experiment, 0.10 g NH_2-MIL-53 (Fe) powder was added to MB aqueous solution of 200 mL, and the initial concentrations were 20 mg L^{-1}, 40 and 60 mg L^{-1}, respectively. The suspension is placed in a conical flask and stirred in an isothermal reciprocating vibrating screen at a speed of 200 rpm. In the appropriate time interval, the homologue was removed from the solution and centrifuged for 8 min at the speed of 6000 rpm to separate the solid object. The residual MB concentration in the centrifugal solution was then measured by UV-*vis* spectrophotometer (WFZUV-2000). The standard calibration curve is then used to calculate the concentration of MB. The adsorption amount of MB on NH_2-MIL-53(Fe) powder was calculated by using the difference between the initial concentration of MB and the concentration after adsorption.

3 RESULTS AND DISCUSSION

3. 1 Characterization of the as-prepared NH_2-MIL-53(Fe)

XRD patterns of the as-prepared NH_2-MIL-53(Fe) are presented in Fig. 1. The main diffraction peaks of the as-prepared sample appeared at approximately 8.9 °, 10.1 °, 14.7 °, 16.7 °, 17.8 °, 24.1 °, and 25.9 °. These diffraction peaks are similar to those of the simulated data from NH_2-MIL-53(Fe) single crystals in the literature[17], indicating that pure products with NH_2-MIL-53(Fe) topology were obtained.

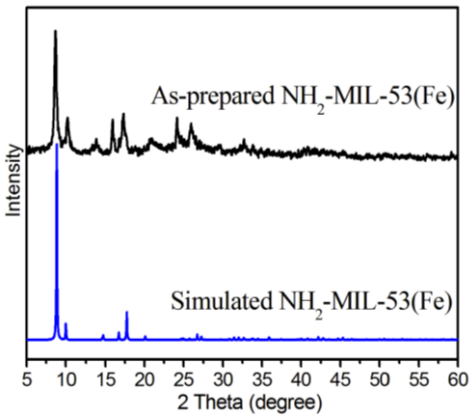

Fig. 1. XRD patterns for the as-prepared and simulated NH_2-MIL-53(Fe) sample

The morphology of the as-prepared sample was surveyed by SEM as displayed in Fig. 2. The SEM photographs (Fig. 2a and Fig. 2b) of NH_2-MIL-53(Fe) samples show that the sample is composed of monodispersed and non-aggregated nanoparticles. The sample shows that the nanoparticles with the morphology of a strip block and size of 200～300 nm in length and 100～120 nm in width.

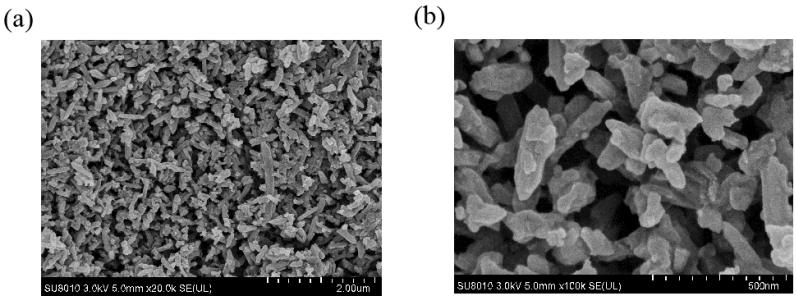

Fig. 2. SEM images for the as-prepared NH_2-MIL-53(Fe) sample

The N_2 adsorption-desorption experiment was conducted to investigate the textural characteristics of the as-prepared NH_2-MIL-53(Fe) sample in Fig. 3. The sample exhibited a type II curve with a H4-type hysteresis loop at intermediate relative pressure (Fig. 3a). The Brunauer-Emmett-Teller (BET) specific surface area of NH_2-MIL-53(Fe) sample is 179.9 $m^2\ g^{-1}$ with a pore volume of 0.29 $cm^3\ g^{-1}$. The porosity of the NH_2-MIL-53(Fe) sample was calculated by Barret-Joyner-Halenda (BJH) method, as shown Fig. 3b, in which the 0.92 nm assigns to the pore diameters of NH_2-MIL-53(Fe) sample, and the 1.7 and 1.95 nm may assign to the aperture between the piled NH_2-MIL-53(Fe) nano-crystals. It is worth mentioning that in addition to micropores (< 2 nm), there are also mesoporous structures (2～50 nm) with different pore sizes in the microstructure of the as-prepared material. This multistage pore structure is helpful to increase the specific surface area and improve the adsorption properties of the material. The total pore volume was calculated to be 0.29 $cm^3\ g^{-1}$.

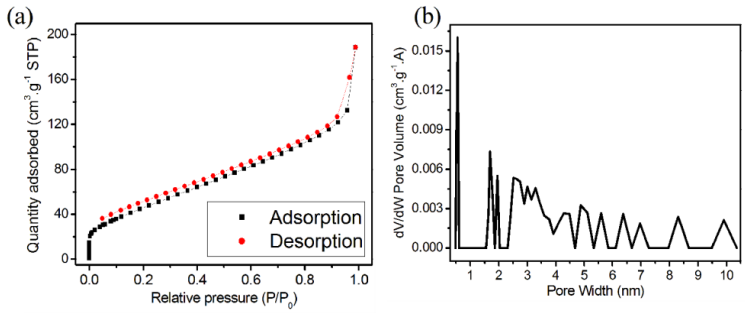

Fig. 3. (a) Nitrogen adsorption-desorption isotherms and (b) pore size distribution curve of the NH_2-MIL-53 (Fe) sample

3. 2 Studies on adsorption kinetics

The curve of adsorption capacity with time is shown in Fig. 4a. It is not difficult to see that the adsorption equilibrium time varies with different initial concentration of dye MB. It is easier to reach adsorption equilibrium at low concentration and longer at high concentration.

In order to design an adsorption treatment plant, it is very important to discuss the adsorptive rate at which contamination is removed from the aqueous solution. In this study, adsorption kinetics was investigated applying four kinetic models, that is, the pseudo-first-order kinetic model and the pseudo-second-order kinetic model.

The pseudo-first-order model equation is applicable for the adsorption of a liquid/solid system based on solid capacity, and is more suitable for lower concentrations of solution, can be expressed by the following linear form[18]:

$$\ln(Q_e - Q_t) = \ln Q_e - k_1 t \qquad (1)$$

Where Q_e and Q_t (mg g^{-1}) are the amounts of adsorbed MB at equilibrium and at time t (min), respectively, and k_1 (1/min) presents pseudo-first-order rate constant. Value of k_1 in the linear form can be calculated from the slope of the plot of $\ln(Q_e - Q_t)$ versus t.

The pseudo-second-order model was commonly applied to calculate the adsorption behavior during the entire adsorption period and is in accordance with the adsorption mechanism of rate controlling steps. The rate of the pseudo-second-order reaction mainly conceptualizes the amount of solute adsorbed on the surface of adsorbent and the amount adsorbed at equilibrium. The pseudo-second-order model can be represented in the following linear form[19]:

$$\frac{t}{Q_t} = \frac{1}{k_2 Q_e^2} + \frac{t}{Q_e} \qquad (2)$$

Where k_2 (g (mg min)$^{-1}$) is pseudo-second-order rate constant, and values of k_2 and Q_e can be determined through data fitting from the intercept and slope of the plot of t/Q_t versus t.

The results of model fitting for the kinetic equations mentioned above are shown in Fig. 4b and Fig. 4c, and the parameters of the experiment and calculation for the kinetic equations are listed in Table 1. For the low concentration solution (20 mg L^{-1}), the linear fitting factor R^2 of the pseudo-first-order kinetic model and the pseudo-second-order kinetic model are relatively high, while for the high concentration solution (40 and 60 mg L^{-1}), the linear fitting factor R^2 of the pseudo-second-order kinetic model is obviously higher than that of the pseudo-first-order kinetic model. In general, compared to the pseudo-first-order kinetic model, the pseudo-second order fitted to the adsorption data better describing the entire adsorption process, and all the values of R^2 are close to 1. There were minimal deviations between the calculated and experimental Q_e values for the pseudo-second-order model, while the calculated Q_e values for the pseudo-first-order model remarkably deviated from the experimental Q_e values.

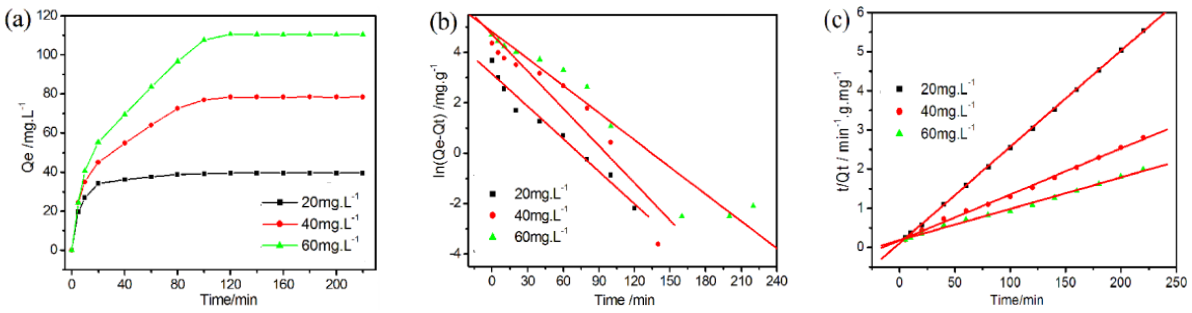

Fig. 4. (a) Effect of initial concentration and contact time on MB adsorption onto NH_2-MIL-53(Fe) adsorbent at room temperature; (b) Model fitting for the four kinetic models: pseudo-first-order kinetic model and (c) pseudo-second-order kinetic model

Table 1. Parameters of the Experiment and Calculation for the Kinetic Equations

[MB] (mg L^{-1})	$Q_{e,exp}$ (mg g^{-1})	Pseudo-first-order kinetic model			Pseudo-second-order kinetic model		
		k_1 (1/min)	$Q_{e1,cal}$ (mg g^{-1})	R^2	k_2 (g (mg min)$^{-1}$)	$Q_{e2,cal}$ (mg g^{-1})	R^2
20	39.65	0.04290	23.04	0.9858	0.00505	40.65	1
40	78.50	0.04912	111.29	0.7484	0.00075	85.32	0.9990
60	110.49	0.03582	124.25	0.7729	0.00035	124.85	0.9987

4 CONCLUSION

In this present study, nanometer block of amide-functionalized Fe(Ⅲ)-based metal-organic frameworks, NH_2-MIL-53(Fe), were prepared via ultrasonic method without any surfactants at room temperature and atmospheric pressure. The characterization for the as-prepared nano-structured MOFs was established by XRD, SEM, XPS, and N_2 adsorption-desorption. The as-prepared sample with high specific surface area (179.9 $m^2 g^{-1}$) showed excellent adsorption for MB in the liquid phase. The as-prepared NH_2-MIL-53(Fe) adsorbent seems to be a promising material in the practice for organic dye removal from aqueous solution.

REFERENCES

(1) Fu, Y.; Viraraghavan, T. Fungal decolorization of dye wastewaters: a review. *Bioresour Technol*. **2001**, 79, 251–262.

(2) Forgacs, E.; Cserháti, T.; Oros, G. Removal of synthetic dyes from wastewaters: a review. *Environ. Int*. **2004**, 30, 953–971.

(3) Sharma, P.; Kaur, H.; Sharma, M.; Sahor, V. A review on applicability of naturally available adsorbents for the removal of hazardous dyes from aqueous waste. *Environ. Monit. Assess* **2011**, 183, 151–195.

(4) Ahmad, A.; Mohd-Setapar, S. H.; Chuong, C. S.; Khatoon, A.; Wani, W. A.; Kumard, R.; Rafatullah, M. Recent advances in new generation dye removal technologies: novel search for approaches to reprocess wastewater. *RSC Adv*. **2015**, 5, 30801–30818.

(5) Guo, H.; Chen, J.; Weng, W.; Zheng, Z.; Wang, D. Adsorption behavior of Congo red from aqueous solution on La_2O_3-doped TiO_2 nanotubes. *J. Ind. Eng. Chem.* **2014**, 20, 3081–3088.

(6) Guo, H.; Ke, Y.; Wang, D.; Lin, K.; Shen, R.; Chen, J. Efficient adsorption and photocatalytic degradation of Congo red onto hydrothermally synthesized NiS nanoparticles. *J. Nanopart. Res.* **2013**, 15, 1475–1486.

(7) Yaghi, O. M.; O'Keeffe, M.; Ockwig, N. W.; Chae, H. K.; Eddaoudi, M.; Kim, J. Reticular synthesis and the design of new materials. *Nature* **2003**, 423, 705–714.

(8) Haque, E.; Lo, V.; Minett, A. I.; Harris, A. T.; Church, T. L. Dichotomous adsorption behaviour of dyes on an amino-functionalised metal-organic framework, amino- MIL-101(Al). *J. Mater. Chem. A* **2014**, 2, 193–203.

(9) Guo, H.; Lin, F.; Chen, J.; Li, F.; Weng, W. Metal-organic framework MIL-125(Ti) for efficient adsorptive removal of Rhodamine B from aqueous solution. *Appl. Organomet. Chem*. **2015**, 29, 12–19.

(10) Guo, H.; Niu, B.; Wu, X.; Zhang, Y.; Ying, S. Effective removal of 2,4,6-trinitrophenol over hexagonal metal-organic framework NH_2-MIL-88B(Fe). *Appl. Organomet. Chem.* **2019**, 33, e4580.

(11) Tranchemontagne, D. J.; Hunt, J. R.; Yaghi, O. M. Room temperature synthesis of metal-organic frameworks: MOF-5, MOF-74, MOF-177, MOF-199, and IRMOF-0. *Tetrahedron* **2008**, 64, 8553–8557.

(12) Guo, H.; Zheng, Z.; Zhang, Y.; Lin, H.; Xu, Q. Highly selective detection of Pb^{2+} by a nanoscale Ni-based metal-organic framework fabricated through one-pot hydrothermal reaction. *Sensor. Actuat. B Chem.* **2017**, 248, 430–436.

(13) Wu, Y.; Wu, X.; Niu, B.; Zeng, Y.; Zhu, M.; Guo, H. Facile fabrication of Ag_2(bdc)@Ag nano-composites with strong green emission and their response to sulfide anion in aqueous medium. *Sensor. Actuat. B Chem.* **2018**, 255, 3163–3169.

(14) Zhu, M.; Wu, X.; Niu, B.; Guo, H.; Zhang, Y. Fluorescence sensing of 2,4,6-trinitrophenol based on hierarchical IRMOF-3 nanosheets fabricated through a simple one-pot reaction. *Appl. Organomet. Chem.* **2018**, 32, e4333.

(15) Khan, N. A.; Jhung, S. H. Synthesis of metal-organic frameworks with microwave or ultrasound: rapid reaction, phase-selectivity, and size reductio, *Coord. Chem. Rev.* **2015**, 285, 11–23.

(16) Nikseresht, A.; Daniyali, A.; Ali-Mohammadi, M.; Afzalinia, A.; Mirzaie, A. Ultrasound-assisted biodiesel production by a novel composite of Fe(III)-based MOF and phosphotangestic acid as efficient and reusable catalyst. *Ultrason. Sonochem.* **2017**, 37, 203–207.

(17) Bauer, S.; Serre, C.; Devic, T.; Horcajada, P.; Marrot, J.; Ferey, G.; Stock, N. High-throughput assisted rationalization of the formation of metal organic frameworks in the iron(III) aminoterephthalate solvothermal system. *Chem.* **2008**, 47, 7568–7576.

(18) Arancibia-Miranda, N.; Silva-Yumi, J.; Escudey, M. Effect of cations in the background electrolyte on the adsorption kinetics of copper and cadmium and the isoelectric point of imogolite. *J. Hazard. Mater*. **2015**, 299, 675–684.

(19) Ho, Y. S.; McKay, G. Pseudo-second order model for sorption processes. *Process Biochem*. **1999**, 34, 451–465.